

COLD-FORMED STEEL COLUMNS SUBJECT TO LOCAL BUCKLING AT ELEVATED TEMPERATURES

S. Gunalan¹, Y. Bandula Heva² and M. Mahendran³

ABSTRACT

Fire safety design of building structures has received greater attention in recent times due to continuing losses of properties and lives in fires. However, the structural behaviour of thin-walled cold-formed steel columns under fire conditions is not well understood despite the increasing use of light gauge steels in building construction. Cold-formed steel columns are often subject to local buckling effects. Therefore a series of laboratory tests of lipped and unlipped channel columns made of varying steel thicknesses and grades was undertaken at uniform elevated temperatures up to 700°C under steady state conditions. Finite element models of the tested columns were also developed, and their elastic buckling and nonlinear analysis results were compared with test results at elevated temperatures. Effects of the degradation of mechanical properties of steel with temperature were included in the finite element analyses. The use of accurately measured yield stress, elasticity modulus and stress-strain curves at elevated temperatures provided a good comparison of the ultimate loads and load-deflection curves from tests and finite element analyses. The commonly used effective width design rules and the direct strength method at ambient temperature were then used to predict the ultimate loads at elevated temperatures by using the reduced mechanical properties. By comparing these predicted ultimate loads with those from tests and finite element analyses, the accuracy of using this design approach was evaluated.

Introduction

Cold-formed steel short columns are susceptible to local and distortional buckling effects. Many cold-formed steel codes, (AS/NZS 4600 2005, Eurocode 3 Part 1.3 2006, BS 5950 Part 5 1998 and AISI S100-07 2007), and the Direct Strength Method (DSM) give suitable design guidelines for cold-formed steel short columns subjected to local buckling at ambient temperature. BS 5950 Part 8 (1990) and Eurocode 3 Part 1.2 (2005) give design guidelines for steel members at elevated temperatures. These two design standards mainly focus on hot-rolled steel members and recommend the same guidelines for the design of cold-formed steel members with some limitations, despite the fact that the behaviour of cold-formed steel members is different from that of hot-rolled steel members. This leads to uneconomical designs for cold-formed steel structures. Distortional buckling behaviour of cold-formed steel members was investigated at ambient temperature by Schafer (2001, 2002, 2006) while further investigations at ambient and elevated temperatures were conducted by Ranawaka (2006), who proposed new design guidelines. However, local buckling behaviour of cold-formed steel members at elevated temperatures is not fully investigated and there is no well documented test data to form design guidelines at elevated temperatures. Therefore a series of local buckling tests was carried out on cold-formed steel short columns at ambient and elevated temperatures.

Many numerical softwares are available to predict the structural behaviour of thin-walled structural members subjected to different actions. These numerical analyses predict accurate results provided the loading and boundary conditions and relevant mechanical properties are modelled correctly. In this research, ABAQUS was used in the finite element analyses of cold-formed steel compression members subject to local buckling. Elastic buckling analyses were first carried out and then nonlinear analyses were carried out to obtain the ultimate load. Appropriate imperfections were included to the most probable buckling modes to initiate the nonlinear analyses. Finite element models were validated using the load-deflection curves, failure mode and ultimate loads obtained from the tests.

¹Associate Lecturer, Science and Engineering Faculty, Queensland University of Technology, Brisbane, QLD 4000

²Former PhD Researcher, Science and Engineering Faculty, Queensland University of Technology, Brisbane, QLD 4000

³Professor, Science and Engineering Faculty, Queensland University of Technology, Brisbane, QLD 4000

This paper describes the preliminary investigation, selection of test specimens, method of testing, and the results. It also presents the details of the finite element models developed to investigate the local buckling behaviour of cold-formed steel compression members and their validation using the experimental test results. Finally it compares the test and FEA results obtained at elevated temperatures with the ultimate load capacities obtained using the reduced mechanical properties, based on existing cold-formed steel standards at ambient temperature.

Experimental Investigation

Two series of experimental investigations were carried out to understand the behaviour of cold-formed steel compression members subject to local buckling at ambient temperature and different elevated temperatures up to 700°C. Elastic local buckling analyses of the chosen sections were undertaken using CUFSM and ABAQUS to ensure the occurrence of local buckling during experiments. These analyses were then extended to elevated temperatures using the reduced mechanical properties of 0.95 mm, 1.9 mm and 1.95 mm thick cold-formed steels from Dolamune Kankanamge (2010) and Dolamune Kankanamge and Mahendran (2011). The first test series was carried out at the ambient temperature and the second test series was carried out at elevated temperatures inside an electrical furnace.

Local Buckling Tests at Ambient Temperature

The first series of experimental investigation and numerical analysis were carried out at room temperature (approximately 20°C). Preliminary investigations were carried out to find suitable test section types, thickness and steel grades of light gauge cold-formed steel commonly used for structural members. These sections were analysed using CUFSM, ABAQUS and design guidelines of AS/NZS 4600 to find the most suitable geometry of test specimens.

Preliminary Investigation and Selection of Test Specimens

Most commonly available sections, lipped and unlipped channels, were selected for the testing (see Fig. 1). However, the chosen section dimensions were not standard sizes to ensure the occurrence of desired buckling failures. A slender web was selected for the lipped channels while slender flanges were selected for the unlipped channels to ensure that local buckling occurred in the web elements of lipped channels and the flange elements of unlipped channels. These buckling modes were also ensured by calculating the effective widths of stiffened and unstiffened elements based on AS/NZS 4600. Specimen lengths were selected as a multiple of half wave lengths. In addition to the above length, an additional 20 mm length was included to either ends to minimize the effect of end supports. Thicknesses of 0.95 mm, 1.90 mm and 1.95 mm were selected with low and high grade steels to represent the light gauge cold-formed steel domain. Table 1 shows the buckling half wave lengths (l) and the chosen specimen lengths for different sections. Table 2 shows the mechanical properties of the selected cold-formed steels at ambient temperature.

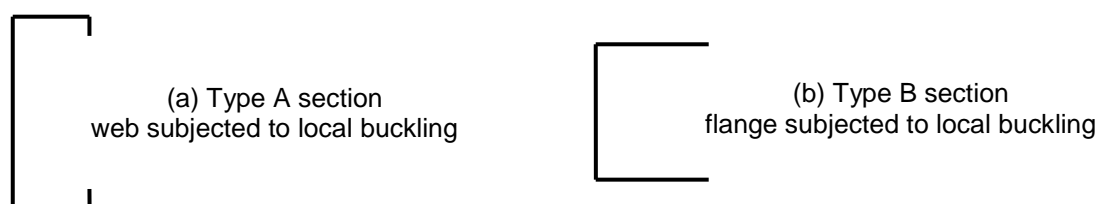


Figure 1. Selected cross section types for local buckling tests.

Table 1. Nominal dimensions of test specimens.

Nominal Thickness (mm)	Grade of steel	Type of section	Web depth (mm)	Flange width (mm)	Lip (mm)	l (mm)	Length of specimens (mm)
0.95	250	A	60	30	9	50	190
		B	25	25		55	150
	550	A	60	25	9	50	190
		B	25	25		55	150
1.95	250	A	118	38	15	90	320
		B	48	49		110	260
1.90	450	A	98	38	15	80	280
		B	48	49		110	260

Table 2. Mechanical properties of the selected cold-formed steels

Steel	f_{y20} (MPa)	E_{20} (MPa)
G550-0.95	615	205000
G250-0.95	320	200000
G450-1.90	515	206000
G250-1.95	271	188000

Test Set-up and Procedure

Ambient temperature tests were conducted using the Tinius Olsen testing machine in the QUT Structural Laboratory (see Fig. 2 (a)). Inbuilt load cells of the machine measure the axial compression load. The specimen was located on the centre of a thicker steel plate, which was located on the base of the testing machine. A similar size steel plate was fixed to the cross-head of the machine. During the tests, two types of displacements, axial shortening and out-of-plane displacements, were recorded (see Fig. 2 (b)). All the LVDTs and the load channel were connected to a data logger system and their readings were recorded during the test (Bandula Heva 2009).

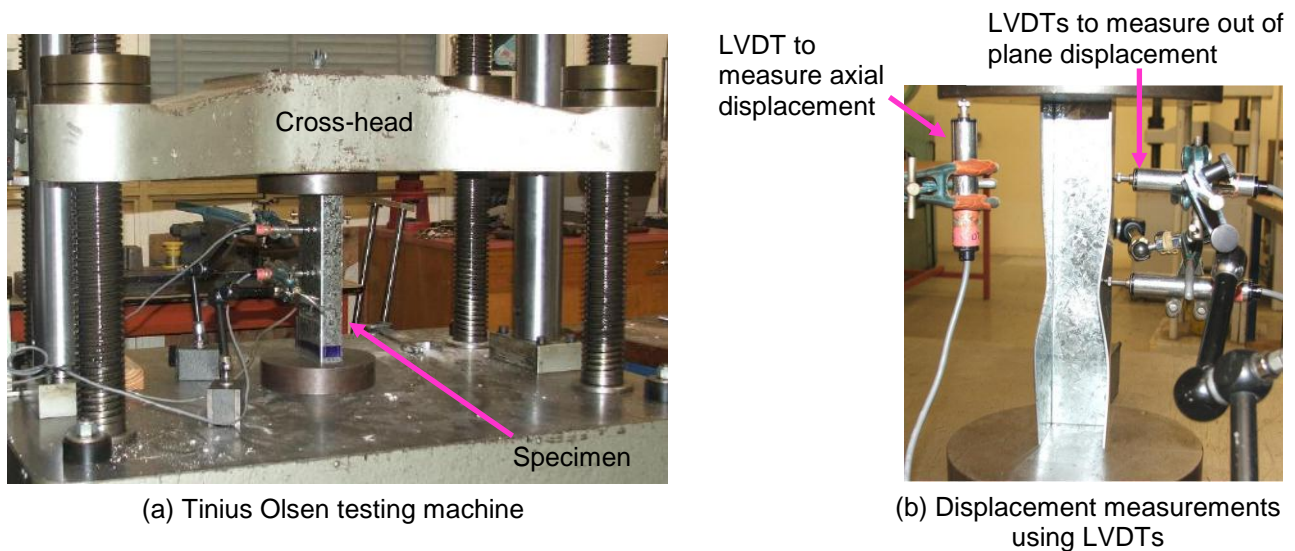


Figure 2. Test set-up at ambient temperature

Observations and Results

Elastic buckling waves were first observed in the tests and their amplitude gradually increased. After reaching the elastic buckling load, axial compression load was further increased owing to the presence of considerable post-buckling capacity. During the post-buckling stage, elastic buckling waves were reduced to a single wave. The maximum load during the test was displayed and recorded by the machine. Also, the ultimate load was confirmed from the peak value of the axial load versus axial shortening curves.

Local Buckling Tests at Elevated Temperature

The second series of tests was conducted to understand the behaviour of cold-formed steel short columns subjected to local buckling at elevated temperatures. Since cold-formed steel members lose their strength significantly after 700°C, these tests were limited to 700°C. The same cold-formed steel section types, thicknesses and grades tested at ambient temperature were used for elevated temperature tests. Most fire design codes follow the method of assessing the capacity at elevated temperatures by using the reduced mechanical properties at elevated temperatures. Therefore, the steady state test method was used in this research where the test specimen was heated to the required temperature and then loaded until failure.

Preliminary Investigation and Selection of Test Specimens

All the selected specimens were analysed to find the elastic buckling loads and buckling modes using CUFSM and ABAQUS at pre-selected temperatures using the reduced mechanical properties reported in Dolamune Kankanamge (2010). The yield strength of cold-formed steel deteriorates rapidly after 500°C.

Hence it is small beyond 600°C compared to the elastic modulus. This results in a lower squash load and a higher elastic buckling load in this range. Therefore it is difficult to find the specimens that show elastic buckling beyond 600°C.

Test Set-up and Procedure

The small electric furnace in the QUT Structural Laboratory was used to heat the specimens (see Fig. 3 (a)) Two holes were provided at the top and bottom of the furnace to insert loading shafts. Special openings on the furnace were used to insert an LVDT and a thermocouple to the specimen. They were used to measure the out-of-plane deflection and the temperature of the specimen. A loading arrangement was made using stainless steel, which gives better performance at elevated temperatures up to 1100°C. Bottom shaft was simply located on the flat base of Tinius Olsen Testing Machine. Top loading shaft was fixed to the cross head of the machine through a rigid plate. Special care was taken to align the loading shafts to avoid eccentric loading.

Test specimen was heated to the required temperature and then allowed another 20 minutes to ensure a uniform temperature throughout the specimen prior to loading. During the heating phase the axial load on the specimen was carefully monitored. Since the thermal expansion of the specimen and loading shafts induced a compression load, the machine cross-head was raised very slowly so that an initial load of 0.1kN was maintained. Finally the load was applied until failure by lowering the upper loading shaft that was attached to the Tinius machine cross-head. The typical failure patterns of Type A and B specimens at elevated temperatures are shown in Figs. 3 (b) and (c), respectively.

Results of Local Buckling Tests at Elevated Temperatures

Both axial compression load versus axial shortening and axial compression load versus out of plane displacement were recorded and plotted. The maximum ultimate load was noted from the display unit of the Testing Machine. The axial compression load versus axial shortening curve at elevated temperature is shown in Fig. 5 for G250-0.95-300-B specimen while Bandula Heva (2009) gives the other load-deflection curves. Tables 3 and 4 give the ultimate loads of Type A and B specimens at elevated temperatures, respectively.

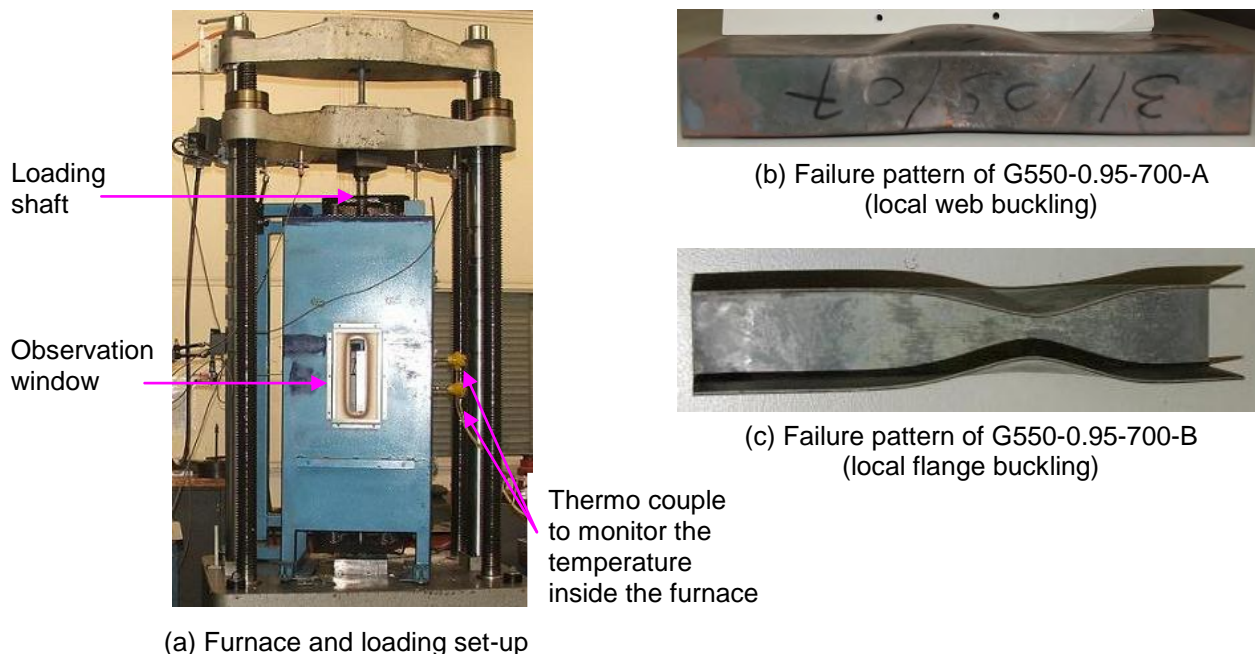


Figure 3. Local buckling tests at elevated temperatures

Development of Finite Element Models

A finite element model of short cold-formed steel column was developed with appropriate boundary conditions to simulate their behaviour at elevated temperatures and to determine the ultimate load capacity. S4 shell element type with a 3 mm x 3 mm mesh size was selected based on detailed convergence studies.

Loading and Boundary Conditions

In finite element analyses, it is important to use accurate boundary conditions to simulate the experimental tests. Hence only axial translation was allowed to the nodes at the upper end of the finite element model. On the lower end, all the translation and rotational movements were restrained. These boundary conditions were applied to the independent node of the rigid fixed MPC (Multi Point Constraint), which was located at the geometric centre of the cross-section. The load was applied to the independent node at the geometric centre of the rigid fixed MPC located at the upper end (see Fig. 4).

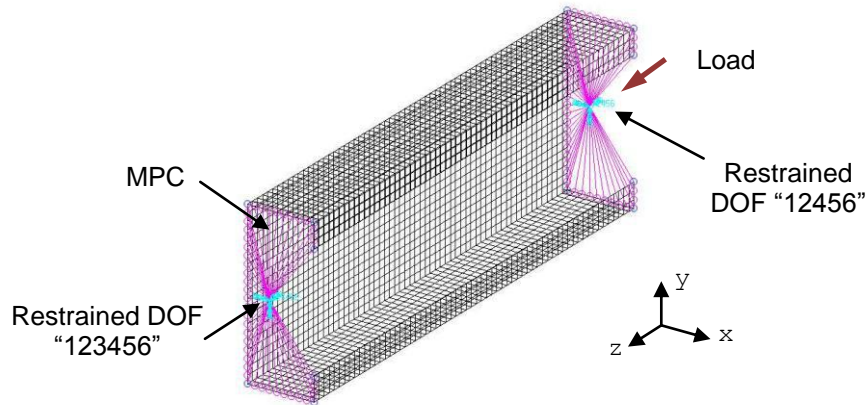


Figure 4. Loading and boundary conditions

Geometric Imperfections and Residual Stresses

Many researchers used the measured imperfections in their finite element simulations (Ranawaka 2006, Sivakumaran and Abdel-Rahman 1998, Dubina and Ungureanu 2002). Some researchers used the section thickness as the value of imperfection for the lipped channels made of thin cold-formed steels (Feng et al. 2003, Chen and Young 2006). Initial imperfection of stiffened elements subjected to local buckling is also taken as a function of the web width. For example, Outinen and Myllymaki (1995) used $h/200$, where h is the width of the stiffened element. Schafer and Pekoz (1998) recommended the initial imperfection of web elements of lipped channel members to be taken as a function of the width of web (w), $0.006w$, or an exponential function based on the thickness (t) of the web as $6te^{-2t}$. Many researchers including Schafer and Pekoz (1998) consider the thickness as the imperfection for plain channels in the case of thinner sections (Ranawaka 2006, Schafer and Pekoz 1998). Camotim et al. (2006) used an amplification factor of $0.15t$ for the imperfection of both local and distortional buckling. After detailed considerations of all the above, the imperfection models proposed by Schafer and Pekoz (1998) for lipped channels ($6te^{-2t}$) and Camotim et al. (2006) for plain channels ($0.15t$) were used because they gave closer predictions in comparison with the experimental ultimate loads.

The residual stress model proposed by Ranawaka (2006) was used in this research. However, the difference between the ultimate load capacities obtained with and without residual stresses was less than 1%. Also the residual stresses reduce with increasing temperatures. Hence it was decided to ignore the effect of residual stresses in the finite element analyses of short columns.

Mechanical Property Model

Mechanical properties are characterized by elastic modulus, stress-strain relationship and Poisson's ratio. There are two stress-strain models, namely elastic-perfect plastic and strain hardening models used in finite element analyses. The stress-strain curves from the tensile coupon tests show the presence of strain hardening behaviour. The use of strain hardening model becomes more important for the elevated temperature simulations because the stress-strain curves at elevated temperatures do not show a clear elastic region. In order to compare the mechanical property models, local buckling behaviour of G550-0.95-500-A specimen was simulated based on elastic-perfect plastic and strain hardening models. Since a clear yielding region was not observed in the stress-strain curves, 0.2% proof stress was considered as the yield stress. The load-deflection curves obtained from these analyses were compared with the load-deflection curves from the experimental test. In the case of elevated temperature simulations at 500°C , the use of strain hardening model gave a better agreement with the test result. Therefore it was concluded that strain hardening mechanical property model must be used to simulate the local buckling behaviour of cold-formed steel columns, particularly at elevated temperatures.

Ambient temperature mechanical properties of G550-0.95 mm and G250-0.95 mm thick cold-formed steels were obtained from Ranawaka and Mahendran (2009) while those for G450-1.90 mm and G250-1.95 mm were obtained from Dolamune Kankanamge (2010). Table 2 gives the ambient temperature mechanical properties for the selected steel thicknesses and strength grades. For G450-1.90 mm and G250-1.95 mm thick cold-formed steels at elevated temperatures, the measured mechanical property values were obtained from Dolamune Kankanamge (2010). For G550-0.95 mm and G250-0.95 mm thick cold-formed steels, they were obtained from the equations proposed by Dolamune Kankanamge and Mahendran (2011) since the measured values were not available. The Ramberg Osgood stress-strain model and appropriate parameters proposed by Ranawaka and Mahendran (2009) and Dolamune Kankanamge and Mahendran (2011) were used. Elevated temperature mechanical properties (f_{yT} and E_T) were used in their proposed equations to derive the stress-strain curves at the required temperatures for use in finite element analyses. The Ramberg Osgood stress-strain model cannot be used for the low strength cold-formed steels at lower temperatures because they show a yield plateau in the stress-strain curves. Therefore the elastic-perfect plastic mechanical property model was used in the finite element analyses of cold-formed steel columns at lower temperatures up to (including) 200°C.

Analysis Methods

As the initial approach, finite strip analyses using CUFSM were carried out to determine the elastic buckling loads and buckling half wave lengths of all the trial sections. The selected specimens were analysed using ABAQUS to determine the elastic buckling and ultimate loads. MSC/PATRAN was used as a pre-processor to create the input files and as a post-processor to read the results. Two types of analyses were carried out using ABAQUS. The bifurcation buckling analysis was used to determine the elastic buckling loads and modes and the nonlinear analysis was used to determine the ultimate loads and deformations. Initial geometric imperfections were included into the appropriate eigen buckling mode from the elastic buckling analyses. Nonlinear analyses were carried out using the modified Riks method to find the ultimate compression load. In the nonlinear analyses, the maximum load increment was controlled appropriately to obtain smooth loading and accurate load factor at failure.

Validation of Finite Element Models

It is important to validate the finite element model developed to simulate the local buckling behaviour. For this purpose, a total of seven finite element models of the tested specimens were simulated at ambient temperature and different elevated temperatures. These seven models consisted of three thicknesses (0.95 mm 1.90 mm and 1.95 mm), two grades (low and high strength steels) and two section types (lipped and unlipped). They were validated using the load-shortening curves, ultimate loads and failure modes.

Load-Shortening Curves

Axial compression load versus axial shortening curves for the tests were obtained from the experimental tests. Same curves were also obtained from the finite element analyses. The load-shortening curves obtained from test and FEA for G250-0.95-300-B specimen are shown in Fig. 5. The load-shortening curves from both tests and FEA showed a good agreement. Therefore it can be concluded that the developed finite element models accurately simulate the local buckling behaviour of cold-formed steel short columns.

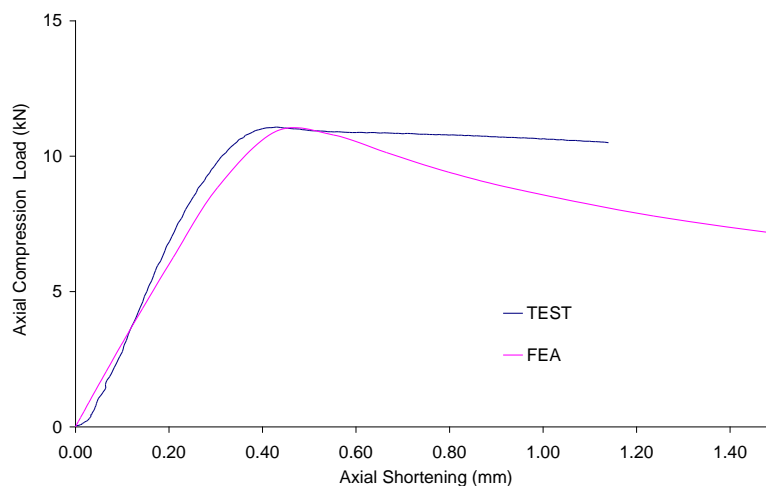


Figure 5. Comparison of load-shortening curves from test and FEA

Ultimate Loads

Both the elastic buckling load and the ultimate load were obtained from the analyses. However, the elastic buckling load could not be measured accurately during testing. Therefore the ultimate load was used to validate the finite element models. Tables 3 and 4 show the comparison of the ultimate loads from tests and FEA for Types A and B specimens, respectively. These tables also summarise the mean values and associated coefficients of variation for the ratio of ultimate loads from test to finite element analyses at different elevated temperatures. The mean values for different cases (steel grade, thickness and type) remained between 0.97 and 1.10, which indicate a good agreement between test and FEA predictions.

Failure Modes

Accuracy of the developed models was also assessed by comparing the failure modes from the finite element analyses and test specimens. The comparison of failure modes for Type A and B specimens are shown in Figs. 6 (a) and (b), respectively. They showed that the failure modes from FEA and experimental tests were very similar. By considering the ultimate loads, load-shortening curves and failure modes, it can be concluded that the developed finite element models are accurate to simulate the local buckling behaviour of cold-formed steel compression members at ambient and elevated temperatures.

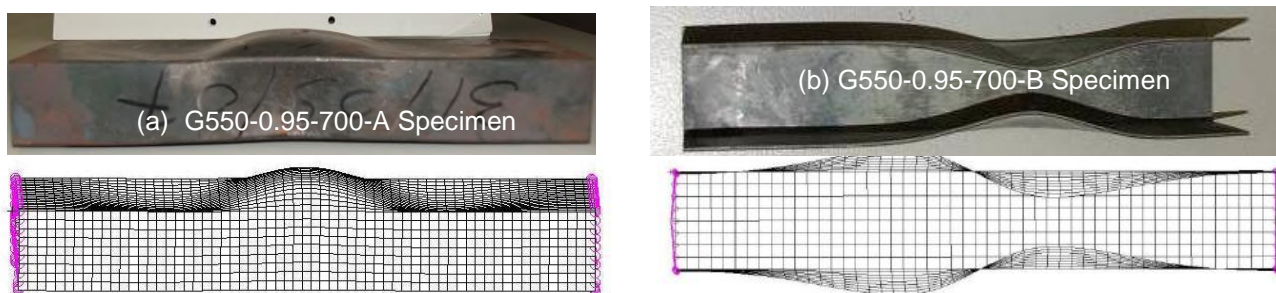


Figure 6. Comparison of failure modes from test and FEA

Table 3. Comparison of ultimate loads from tests, FEA and design standards for Type A sections

Specimen	Temp. (°C)	Test (kN)	FEA (kN)	Test/FEA	Test/Predicted			
					EC3 P1.2	AS/NZS 4600	BS 5950	DSM
G550 0.95 A	20	53.95	55.00	0.98	1.11	1.14	1.02	1.10
	100	53.47	54.40	0.98	1.10	1.14	1.01	1.12
	200	52.12	52.70	0.99	1.08	1.11	0.99	1.13
	300	47.83	48.40	0.99	1.04	1.07	0.95	1.13
	400	36.43	35.70	1.02	1.08	1.11	0.99	1.14
	500	21.36	21.80	0.98	1.13	1.16	1.03	1.06
	600	6.55	7.01	0.93	1.22	1.26	1.12	0.85
	700	4.00	4.38	0.91	1.18	1.21	1.08	0.85
	Mean			0.97	1.118	1.149	1.026	1.047
	COV			0.03	0.052	0.052	0.053	0.118
G450 1.90 A	20	151.30	162.0	0.93	1.01	0.97	0.97	0.99
	300	146.18	141.00	1.04	1.04	1.00	1.00	1.11
	500	70.10	59.90	1.17	1.22	1.17	1.18	1.20
	600	23.65	19.80	1.19	1.44	1.39	1.39	1.10
	700	11.64	11.50	1.01	1.17	1.12	1.13	0.95
	Mean			1.07	1.175	1.130	1.136	1.069
	COV			0.10	0.147	0.148	0.147	0.097
G250 1.95 A	20	102.04	105.00	0.97	1.04	1.04	1.06	1.01
	300	80.92	72.30	1.15	1.15	1.14	1.16	1.07
	400	61.60	53.60	1.15	1.16	1.16	1.18	1.06
	500	37.58	34.90	1.08	1.09	1.09	1.11	0.96
	600	23.00	20.50	1.12	1.19	1.18	1.21	1.00
	700	14.86	12.90	1.15	1.21	1.21	1.23	1.07
	Mean			1.10	1.140	1.136	1.156	1.027
	COV			0.06	0.056	0.055	0.055	0.045

Note – Test results are not available for G250-0.95-A specimens

Table 4. Comparison of ultimate loads from tests, FEA and design standards for Type B sections

Specimen	Temp. (°C)	Test (kN)	FEA (kN)	Test/FEA	Test/Predicted			
					EC3 P1.2	AS/NZ S 4600	BS 5950	DSM
G550 0.95 B	20	26.50	29.00	0.91	1.06	1.07	1.14	0.96
	200	26.36	27.30	0.97	1.06	1.07	1.14	1.02
	300	25.91	25.00	1.04	1.09	1.10	1.17	1.10
	400	22.08	18.70	1.18	1.27	1.28	1.36	1.23
	500	14.32	11.30	1.27	1.47	1.47	1.57	1.27
	600	4.15	3.94	1.05	1.51	1.51	1.61	0.97
	700	2.02	2.44	0.83	1.15	1.16	1.24	0.77
	Mean			1.03	1.230	1.237	1.319	1.045
	COV			0.15	0.155	0.154	0.154	0.165
G250 0.95 B	20	16.83	17.80	0.95	1.10	1.11	1.18	0.95
	200	16.07	15.90	1.01	1.15	1.17	1.23	1.02
	300	10.70	11.00	0.97	1.06	1.08	1.14	0.89
	400	9.25	8.01	1.15	1.27	1.28	1.35	1.02
	500	7.85	5.69	1.38	1.53	1.55	1.63	1.20
	600	3.64	3.96	0.92	1.07	1.08	1.14	0.82
	700	2.22	2.28	0.97	1.17	1.18	1.25	0.90
	Mean			1.05	1.193	1.207	1.274	0.970
	COV			0.16	0.137	0.137	0.137	0.126
G450 1.90 B	20	96.89	101.00	0.96	1.10	1.11	1.20	1.00
	200	86.39	99.70	0.87	0.99	1.00	1.08	0.95
	300	86.10	87.20	0.99	1.04	1.05	1.13	1.04
	400	58.49	66.10	0.88	0.95	0.95	1.03	0.92
	500	35.75	37.50	0.95	1.06	1.07	1.15	0.97
	600	14.00	13.00	1.08	1.45	1.46	1.58	0.99
	700	8.06	7.38	1.09	1.38	1.39	1.50	1.03
	Mean			0.97	1.140	1.148	1.237	0.987
	COV			0.09	0.173	0.173	0.173	0.042
G250 1.95 B	20	66.37	65.50	1.01	1.20	1.22	1.28	1.02
	200	69.60	61.50	1.13	1.33	1.35	1.41	1.14
	300	42.74	44.80	0.95	1.07	1.08	1.13	0.87
	400	36.53	33.20	1.10	1.21	1.23	1.29	0.97
	500	22.69	21.90	1.04	1.16	1.18	1.24	0.89
	600	15.10	13.00	1.16	1.38	1.39	1.46	1.01
	700	9.24	8.19	1.13	1.33	1.34	1.41	1.02
	Mean			1.08	1.240	1.256	1.319	0.988
	COV			0.07	0.089	0.088	0.089	0.093

Comparison of Test and FEA Results with Predictions from the Current Design Standards

Current Design Standards

Many cold-formed steel design codes, (AS/NZS 4600, AISI S100 and BS 5950 Part 5), give design guidelines for cold-formed steel short columns subjected to local buckling at ambient temperature. However, AS/NZS 4600 and AISI S100 give identical guidelines for local buckling. Therefore our test results were compared with the predictions of AS/NZS 4600 and BS 5950 Part 5, which recommend the use of the well known effective width method for local buckling. Therefore our test results were compared with the predictions of these standards. Recently Schafer (2001) proposed the new Direct Strength Method (DSM) that eliminates the tedious calculations of effective width of each plate element in the section. Although the above design codes were originally developed for calculating the local buckling capacities at ambient temperature conditions, the same design equations were used in this research to calculate the local buckling capacities at elevated temperatures, simply by using the appropriately reduced mechanical properties. The mechanical properties used here were the same as those used in the finite element analyses.

Eurocode 3 Part 1.2 (ECS, 2005), AS/NZS 4600 (SA, 2005) and BS 5950 Part 5 (BSI, 1998) use the effective width method to find the local buckling capacity. However, the fire code, Eurocode 3 Part 1.2, recommends the use of effective width at ambient temperature with the yield stress at the elevated

temperature. Therefore the effective areas were calculated based on ambient temperature properties. However, all other design recommendations of these design standards were used with reduced mechanical properties at elevated temperatures. The direct strength method needs the relevant elastic buckling load from a rational buckling analysis. Therefore finite element analyses were carried out using ABAQUS to find the elastic buckling load of tested specimens. Tables 3 and 4 compare the ultimate loads (capacity) from the tests and various design standards for Type A and B specimens, respectively.

Comparison of Test and FEA Results with Code Predictions

According to Eurocode 3 Part 1.2, AS/NZS 4600 and BS 5950 Part 5, the mean ratios for Type A and B specimens are greater than one for all cases (see Tables 3 and 4). This implies that these design codes can be safely used to predict the capacities of cold-formed steel columns with stiffened and unstiffened elements that are subjected to local buckling failures at elevated temperatures, even though they are slightly uneconomical in some cases. The direct strength method predictions are higher than those obtained from other design standards. The test to predicted ratios are mostly less than one. This implies that the direct strength method predictions at elevated temperatures are slightly unsafe for cold-formed steel members with unstiffened elements. In this study, web elements of lipped channels and the flange elements of unlipped channels are slender while all other elements are compact. Since the direct strength method discourages the use of highly slender elements, it may not be accurate enough to predict the local buckling capacity. The direct strength method considers the elastic buckling load of the entire section instead of using the conservative buckling coefficient values of individual elements ($k = 0.43, 4$) as with the effective width based design method. This leads to higher column capacities than the other design standards.

The ultimate loads obtained from the finite element analyses were also compared with the code predictions. However, they are not shown here due to limited space. The ratios of finite element analysis results to the code predictions showed a better consistency compared to the comparison of test results. The mean values of AS/NZS 4600 and BS 5950 Part 5 predictions for Types A and B were close to one while the associated coefficients of variation were small.

Conclusions

Local buckling behaviour and strength of cold-formed steel members was investigated using tests at ambient and elevated temperatures. Cold-formed steel sections made of thinner (0.95 mm) and comparatively thicker (1.90 mm and 1.95 mm) steels were selected with both low and high strength grades. A total of 27 ambient temperature tests were conducted in this study while 64 tests were conducted at elevated temperatures. Finite element models were also developed to simulate the local buckling behaviour and strength of cold-formed steel lipped and unlipped channels under axial compression at ambient and elevated temperatures. The developed finite element models were validated using the ultimate loads, failure modes and load-deflection curves from the experimental tests. The test and FEA results were then compared with the predictions of Australian, American, British and European steel design standards and the direct strength method. A comparative study undertaken in this research showed that these design guidelines can be safely used to predict the local buckling capacities at elevated temperatures using the reduced mechanical properties at these temperatures. The direct strength method predictions were closer to the test results. However, it is slightly unconservative for some sections.

Acknowledgements

The authors would like to thank Australian Research Council for their financial support and the Queensland University of Technology for providing the necessary facilities and support to conduct this research project.

References

- American Iron and Steel Institute (AISI), 2007, *Specifications for the Cold-formed Steel Structural Members, Cold-formed Steel Design Manual*, Washington, USA.
- Bandula Heva, Y., 2009, Behaviour and design of cold-formed steel compression members at elevated temperatures, *Ph.D. Thesis*, Queensland University of Technology, Brisbane, Australia.
- British Standards Institute (BSI), 1990, *BS 5950, Part 8, Structural Use of Steelwork in Building, Code of Practice for Fire Resistance Design*, London, UK.
- Camotim, D., Silvestre, N., Goncalves, R. and Dinis, P.B., 2006, GBT-based structural analysis of thin-walled members: overview, recent progress and future developments, *advances in engineering structures*,

Mechanics and Construction, 187-204.

- Chen, J. and Young, B., 2006, Design of cold-formed steel lipped channel columns at elevated temperatures, *Engineering Structures*, 29, 2445-2456.
- Dolamune Kankanamge, N., 2010, Structural behaviour and design of cold-formed steel beams at elevated temperatures, *Ph.D. Thesis*, QUT, Brisbane, Australia.
- Dolamune Kankanamge, N. and Mahendran, M., 2011, Mechanical properties of cold-formed steels at elevated temperatures, *Thin-Walled Structures*, 49, 26-44.
- Dubina, D. and Ungureanu, V., 2002, Effect of imperfections on numerical simulation of instability behaviour of cold-formed steel members, *Thin-Walled Structures*, 40 (3), 239-262.
- European Committee for Standardization (ECS), *EN 1993-1-2, 2005, Eurocode 3: Design of steel structures. Part 1.2: General Rules - Structural Fire Design*, Brussels, Belgium.
- European Committee for Standardization (ECS), *EN 1993-1-3, 2006, Eurocode 3: Design of Steel Structures. Part 1.3: General Rules - Supplementary Rules for Cold-formed Members and Sheeting*, Brussels, Belgium.
- Feng, M., Wang, Y.C. and Davies, J.M., 2003, Structural behaviour of thin-walled short steel channel columns at elevated temperatures. Part 2: Design calculations and numerical analyses, *Thin-Walled Structures*, 41 (6), 571-594.
- Outinen, T.A. and Myllymaki, J., 1995, The local buckling of RHS members at elevated temperatures, *VIT Research Notes 1672*, Technical Research Centre of Finland, Espoo, Finland.
- Ranawaka, T., 2006, Distortional buckling behaviour of cold-formed steel compression members at elevated temperatures, *Ph.D. Thesis*, Queensland University of Technology, Brisbane, Australia.
- Ranawaka, T. and Mahendran, M., 2009, Experimental study of the mechanical properties of light gauge cold-formed steels at elevated temperatures, *Fire Safety Journal*, 44 (2), 219-229.
- Schafer, B.W. and Pekoz, T., 1998, Computational modelling of cold-formed steel: Characterising geometric imperfections and residual stresses, *Journal of Constructional Steel Research*, 47, 193-210.
- Schafer, B.W., 2001, Thin-walled column design considering local, distortional and euler buckling, *Proceeding of the Structural Stability Research Council Annual Stability Conference*, Ft. Lauderdale, Florida, USA, 419-438.
- Schafer, B.W., 2002, Local, distortional and euler buckling of thin-walled columns, *Journal of Structural Engineering*, 128 (3), 289-299.
- Schafer, B.W., 2006, Progress on the direct strength method, *Proceedings of the Sixteenth International Specialty Conference on Cold-formed Steel Structures*, 647-662
- Sivakumaran, K.S. and Abdul-Rahman, N., 1998, A finite element analysis model for the behaviour of cold-formed steel members, *Thin-Walled Structures*, 31 (4), 305-324.
- Standards Australia (SA), 2005, *AS/NZS 4600, Cold-formed Steel Structures*, Sydney, Australia.
- Yu, W.W., 2000, *Cold-formed Steel Design*, John Wiley & Sons, New York, USA.